CrystEngComm

Accepted Manuscript

ROYAL SOCIETY OF CHEMISTRY

www.rsc.org/crystengcomm

Reversible adsorption and separation of chlorocarbons and BTEX based on Cu(II)-metal organic framework†

Fan Yang,‡ Qi-Kui Liu,‡ Jian-Ping Ma, Yan-An Li, Ke-Xin Wang, and Yu-Bin Dong*

College of Chemistry, Chemical Engineering and Materials Science, Collaborative Innovation Center of Functionalized Probes for Chemical Imaging in Universities of Shandong, Key Laboratory of Molecular and Nano Probes, Ministry of Education, Shandong Normal University, Jinan 250014, P. R. China; E-mail: yubindong@sdnu.edu.cn

Abstract A new non-interpenetrating 2D Cu(II)-metal organic framework has been successfully synthesized from the carbazole-bridging organic ligand **L** and $Cu(NO_3)_2$ in solution. The $Cu\mathbf{L}_2(NO_3)_2$ framework contains square-like channels and the n-butyl groups on **L** face toward the channel center to from the typical hydrophobic pores. In addition, the reported $Cu\mathbf{L}_2(NO_3)_2$ host can reversibly upload various VOCs such as CH_2Cl_2, $CHCl_3$ and BTEX (benzene, toluene, ethylbenzene, *o*-xylene, *m*-xylene, and *p*-xylene) under ambient conditions without loss of framework integrity. Furthermore, it is able to effectively separate CH_2Cl_2 from $CHCl_3$, benzene from toluene/ethylbenzene/xylene and toluene from ethylbenzene/xylene in liquid phase. The selectivity for chlorocarbons is derived from the substrate polarity, while the host-guest hydrophobic interaction might be the dominating factor for BTEX affinity.

Introduction

Chlorocarbons (CH_2Cl_2, $CHCl_3$ and CCl_4) and BTEX (benzene, toluene, ethylbenzene and xylene) are very important materials in organic industrial chemistry. Recent study indicates that these high volatile organic compounds (VOCs) are of great social and environmental significance.[1-2] For example, halocarbons can cause chemical and radiative change in the atmosphere. On the other hand, BTEX are widely used in the manufacture of paints, agricultural chemicals, artificial rubber and chemical intermediates, which results in the BTEX species widely existing in water, air, soil and sediments. These compounds, however, often coexist with their aliphatic or aromatic analogues, and some of them have very similar boiling points. So the enrichment and separation of these organic species is high value,[3] although it is a technical challenge.

Metal-organic frameworks (MOFs),[4] as an emerging class of hybrid porous materials, exhibit a promising application for molecular adsorption and separation.[5] In principle, suitable MOFs with well-defined inner pores and desired functionalized microenvironment could be obtained by subtly designed organic ligands and metal ions, for example hydrophobic or hydrophilic pores. Additionally, adsorption separation based on MOF adsorbents might be a more energy efficient approach than that of distillation, so the development of new types of MOF adsorbents is very significant. Up to date, a series of novel MOFs which are able to effectively adsorb and separate these VOCs have been synthesized,[6] the new porous MOFs, however,

must be synthesized and the reaction chemistry leading to them investigated to generate a sufficiently large database from which MOFs for real practical separation materials can be deduced.

In this contribution, we report a new porous Cu(II)-MOF which is generated from a carbazole-bridged n-butyl-attached organic ligand (**L**) and $Cu(NO_3)_2$. Furthermore, it is able to reversibly absorb and effectively separate CH_2Cl_2/$CHCl_3$/CCl_4 and BTEX under ambient conditions.

Experimental Section

Chemicals and Instruments

All the chemicals were obtained from commercial sources and used without further purification. Infrared (IR) spectrums were obtained in the 400-4000 cm^{-1} range using a Bruker ALPHA FT-IR Spectrometer. Elemental analyses were performed on a Perkin-Elmer model 2400 analyzer. ^1H NMR data were collected on an AM-300 and Varian Advance 600 spectrometer. Chemical shifts are reported in δ relative to TMS. All crystal data were obtained by Agilent SuperNova X-Ray single crystal diffractometer. GC-MS analysis data were performed on a J&K S011525-300 gas chromatographic (Agilent 6890GC-5973MS). The separation data were obtained by Agilent 1260 Infinity HPLC system equipped with an Agilent C18 reverse phase column (150 × 4.6 mm, 5 μm). Thermogravimetric analyses were carried out on a TA Instrument Q5 simultaneous TGA under flowing nitrogen at a heating rate of

10°C/min. XRPD patterns was obtained on D_8 Advance X-ray powder diffractometer with Cu Kα radiation (λ = 1.5405 Å).

Synthesis of 2, 7-dibromo-N-butylcarbazole. n-Butyl bromide (4.01 g, 35 mmol) was added dropwise to the DMF solution of 2,7-Dibromocarbazole (9.75 g, 30 mmol) and NaH (60%, 1.60 g, 40 mmol). The mixture was stirred at room temperature for 10 h. After addition of water (300 mL), the obtained white precipitate was purified by column on silica gel using hexane/methylene chloride (4:1 v/v) as the eluent to afford the product as a white crystalline solid. Yield, 10.50 g, 92 %. IR (KBr pellet cm^{-1}): 2924.49(ms), 2863.60(w), 1578.89(ms), 1481.54(ms), 1420.70(s), 1369.53(w), 1049.83(ms), 992.53(w), 891.31(ms), 731.58(s), 659.36(w), 551.91(w). ^{1}H NMR (300MHz, DMSO, 25°C, TMS): 8.09-8.12 (d, J = 8.3Hz, 2H, -C_6H_3Br), 7.88 (s, 2H, -C_6H_3Br), 7.33-7.36 (d, J = 8.3Hz, 2H, -C_6H_3Br), 4.36-4.40 (t, J = 7.0Hz, 2H, -C_4H_9), 1.66-1.71 (m, J = 30.0Hz, 2H, -C_4H_9), 1.22-1.32 (m, J = 14.8Hz, 2H, -C_4H_9), 0.84-0.89 (t, J = 7.3Hz, 3H, -C_4H_9). Elemental Analysis (%) Calcd. for $C_{16}H_{15}NBr_2$: C 50.39, H 3.94, N 3.67 %. Found: C 50.80, H 4.03, N 3.72%.

Synthesis of L. A mixture of 2, 7-dibromo-N-butylcarbazole (3.81 g, 10 mmol), 1, 2, 4-triazole (1.93 g, 28 mmol), CuI (0.77 g, 4 mmol) and Cs_2CO_3 (13.00 g, 40 mmol) in DMF (20 mL) was heated at 110°C for 36 h. After addition of water, the obtained white precipitate was purified by column on silica gel using methylene chloride/EtOAc (1:1 v/v) as the eluent to afford the product as a white crystalline solid. Yield, 2.1 g, 60 %. IR (KBr pellet cm^{-1}): 3105.89(w), 2961.61(w), 2926.21(w),

1602.34(ms), 1505.41(s), 1406.67(vs), 1402.51(w), 1355.00(ms), 1329.38(ms), 1276.25(s), 1215.01(vs), 1048.13(ms), 996.45(s), 951.20(ms), 795.23(vs), 748.68(w), 669.32(vs), 441.33(w). ^{1}H NMR (300 MHz, DMSO, 25°C, TMS): 9.41 (s, 2H, -$C_2N_3H_2$), 8.35-8.38 (d, J = 6.0 Hz, 2H, -C_6H_3), 8.28 (s, 2H, -$C_2N_3H_2$), 8.28 (s, 2H, -C_6H_3), 7.73-7.76 (d, J = 8.4 Hz, 2H, -C_6H_3), 4.44-4.51 (t, J = 6.1 Hz, 2H, -C_4H_9), 1.79-1.83 (m, J = 27.0 Hz, 2H, -C_4H_9), 1.34-1.36 (m, J = 7.7 Hz, 2H, -C_4H_9), 0.87-0.92 (t, J = 7.1 Hz, 3H, -C_4H_9). Elemental Analysis (%) Calcd. for $C_{20}H_{19}N_7$: C 67.22, H 5.32, N 27.45 %. Found: C 67.00, H 5.45, N 27.55 %.

Synthesis of 1. A solution of $Cu(NO_3)_2$ (8.0 mg, 0.04 mmol) in MeOH (8 mL) was carefully layered on a solution of **L** (10.7 mg, 0.03 mmol) in CH_2Cl_2 (8 mL). The solution was left for about 3 days at room temperature, and green-blue crystals of **1** ([Cu**L**$_2$(NO_3)$_2$]·1.75CH_2Cl_2·CH_3OH) were obtained. Yield: 63 % (based on **L**). IR (KBr pellet, cm^{-1}): 3108.93(w), 2927.86(w), 2866.92(w), 1603.19(ms), 1517.44(s), 1464.48(s), 1401.63(w), 1274.80(vs), 1212.59(ms), 1136.60(ms), 1140.71(w), 991.77(s), 895.33(ms), 797.52(s), 730.57(w), 688.46(s), 624.45(w). ^{1}HNMR (600 MHz, DMSO, 25°C, TMS): 10.48 (s, 2H, -triazole), 9.00 (s, 2H, -triazole), 8.37-8.38 (d, J = 24.0 Hz, 2H, -C_6H_3), 8.16-8.17 (d, 36.0 Hz, 2H, -C_6H_3), 7.78 (s, 2H, -C_6H_3), 4.50-4.51 (t, J = 18.0 Hz, 2H, -C_4H_9), 1.80-1.81 (m, 2H, -C_4H_9), 1.35-1.36 (m, 2H, -C_4H_9), 0.89-0.91 (t, J = 6.0 Hz, 3H, -C_4H_9), 5.76 (s, CH_2Cl_2), 3.16 (s, CH_3OH). The encapsulated guest molecules are not very stable in the pores and can gradually escape from the pores at ambient temperature, so the elemental analysis was

performed on the completely desolvated sample $Cu\mathbf{L}_2(NO_3)_2$. Anal. calcd for $C_{40}H_{38}CuN_{16}O_6$: C 53.24, H 4.20, N 24.84 %. Found: C 53.81, H 4.51, N 24.16 %.

X-ray Crystallography. The X-ray diffraction data for single crystal of **1** was measured at 173 K on an Agilent Technologies Super Nova Single Crystal Diffractometer with graphite-monochromatic Mo Kα radiation (λ = 0.71073 Å). Corrections for incident and diffracted beam absorption effects were applied using CrysAlisPro.[7] None of the crystals showed evidence of crystal decay during data collection. The structures were solved by direct methods using SHELXS program and refined by full matrix least-squares on F^2 including all reflections (SHELXL97).[8] The crystal data, refinement parameters and bond lengths and angles are summarized in Tables 1 - 2.

Table 1. Crystal data and structural refinement parameters for **1**.

Empirical formula	$C_{42.75}H_{46.50}Cl_{3.50}CuN_{16}O_{7.50}$ (**1**)
Formula weight	1092.07
Crystal system	Monoclinic
a (Å)	16.527(11)
b (Å)	20.962(14)
c (Å)	16.969(12)
α (°)	90
β (°)	106.983(10)
γ (°)	90
V (Å^3)	5622(7)

Space group	*P2(1)/c*
Z value	4
ρ calc. (g/cm^3)	1.290
μ (Mo Kα)(mm^{-1})	0.614
Temp(K)	173(2)
F(000)	2254
GOF	1.069
Data / restraints / parameters	9945 / 72 / 743
Reflections collected / unique	27725 / 9945 [R(int) = 0.0794]
Final R indices [I>2sigma(I)]: *R; R_w*	0.0932, 0.2646

[a] $R1 = \Sigma \, ||F_o| - |F_c|| \, / \, \Sigma \, |F_o|$. $wR2 = \{ \Sigma \, [w(F_o^2 - F_c^2)^2] \, / \, \Sigma \, [w(F_o^2)^2] \}^{1/2}$

Table 2. Interatomic distances (Å) and bond angles (°) with esds () for **1**.

Cu(1)-N(1)	1.995(4)	Cu(1)-N(13)#1	2.011(4)
Cu(1)-N(8)	2.039(5)	Cu(1)-N(7)#2	2.050(5)
Cu(1)-O(2)	2.265(8)		

N(1)-Cu(1)-N(13)#1	174.6(2)	N(1)-Cu(1)-N(8)	91.3(2)
N(13)#1-Cu(1)-N(8)	89.4(2)	N(1)-Cu(1)-N(7)#2	90.71(19)
N(13)#1-Cu(1)-N(7)#2	87.09(19)	N(8)-Cu(1)-N(7)#2	163.6(2)
N(1)-Cu(1)-O(2)	96.3(3)	N(13)#1-Cu(1)-O(2)	88.4(3)
N(8)-Cu(1)-O(2)	109.7(3)	N(7)#2-Cu(1)-O(2)	86.2(3)

Symmetry transformations used to generate equivalent atoms: #1 -x+1,y-1/2,-z+3/2 #2 -x,y-1/2,-z+5/2 #3 -x,y+1/2,-z+5/2 #4 -x+1,y+1/2,-z+3/2

Results and discussion

Synthesis and structural analysis

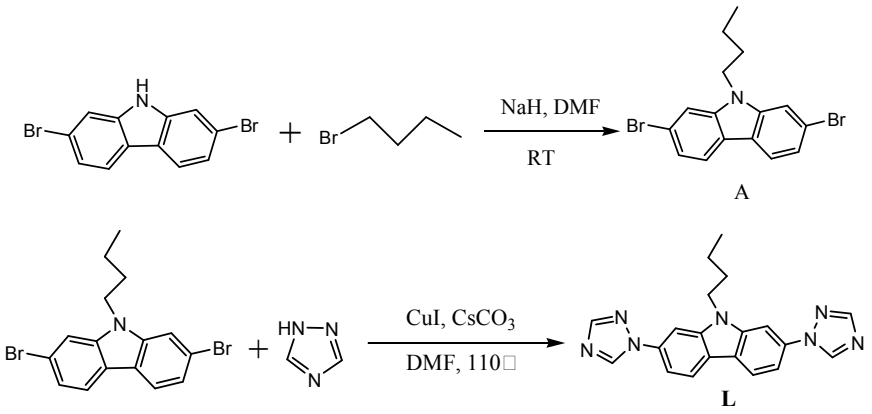

Scheme 1. Synthesis of **L**.

The n-butyl-attached ligand of **L** was simply prepared by the combination of 2, 7-dibromo-N-butylcarbazole and 1, 2, 4-triazole in DMF at 110°C in the presence of CuI/$CsCO_3$ in good yield. Reaction of **L** with $Cu(NO_3)_2$ in a CH_2Cl_2/MeOH mixed solvent system to generate blue crystals of **1** ($[CuL_2(NO_3)_2]\cdot 1.75CH_2Cl_2\cdot CH_3OH$) in 63 % yield. The formula of **1** was established based on single-crystal X-ray diffraction study and thermal gravimetric analysis (TGA, Supporting Information). The XRPD pattern of **1** indicates that the compound was obtained in pure phase (Supporting Information).

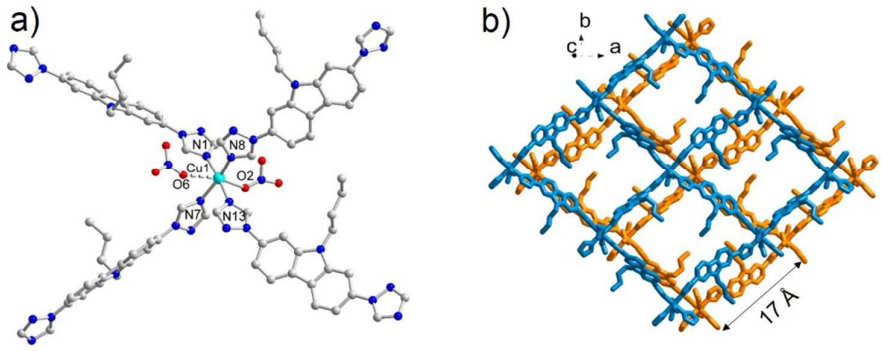

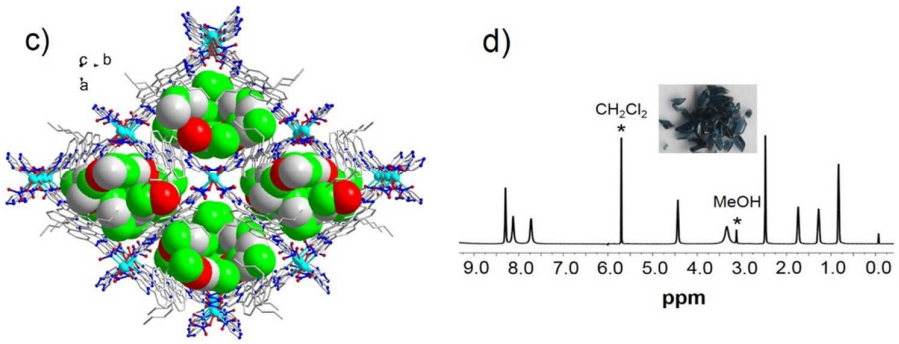

Figure 1. a) Cu(II)-coordination environment in **1** (single-crystal analysis indicated that the coordinated nitrate is disordered, and only major disorder components are shown) b) 2D layer stack together in an -ABAB- fashion. The different net are shown in different color for clarity. c) The crystal packing of **1**. The disordered encapsulated guest molecules are shown as space-filling model. d) ^{1}H NMR spectrum of **1**. The CH_2Cl_2 and MeOH signals are marked for clarity. The photograph of sample **1** was inserted.

X-ray single-crystal analysis revealed that compound **1** crystallizes in the monoclinic space group *P2(1)/c* (Table 1). As shown in Figure 1, each Cu(II) node lies in a distorted octahedral coordination environment which consists of four N atoms from four **L** ligands in the equatorial plane and two O atoms from two NO_3^- anions in the axial positions. The Cu-N bond lengths vary from 1.995(4)-2.050(5) Å. The Cu(1)-O(2) bond length is 2.306(3) Å, while the Cu(1)-O(6) bond length is 2.841(5) Å, indicating the existence of very weak interactions between this nitrate oxygen atom and Cu(II) center. As a node, each Cu(II) atom connects to four adjacent Cu(II) atoms via four bidentate **L** ligands, forming a 4-connected (4, 4) network structure. The 2D layered net contains a square-like window with a Cu···Cu distance of ca. 17 Å (Figure 1).

Furthermore, two sets of 2D nets stack together alternatively along the crystallographic *c* axis in an -ABAB- fashion to generate square-like channels. On the further inspection, we found that all the attached n-butyl groups face toward the center of the channels to form the hydrophobic pores. As shown in Figure 1, 1D square-like channels are full-loaded with CH_2Cl_2 and MeOH solvent molecules. The ^{1}H NMR (DMSO-d^6) spectrum on **1** further confirmed that the existence of CH_2Cl_2 and MeOH guests in **1** (Figure 1).

Reversible adsorption of chlorocarbons and BTEX

Notably, the experiments demonstrated that **1** is able to reversibly upload guest species in liquid phase. The guest-free host framework of **1** was obtained by heating of the crystals at 110°C for 1.5 hours (monitored by the TGA measurement) or extracting with acetonitrile at ambient temperature. The ^{1}H NMR (DMSO-d^6) spectrum on the desolvated sample **1'** clearly indicated that the guest molecules were completely removed, meanwhile the color of the sample changed from blue to green (Figure 2). The corresponding solid **1'** displayed that the shapes and intensities of reflections are almost identical to that of **1**, meaning that guest loss did not result in symmetry change or cavity volume collapse (Supporting Information).

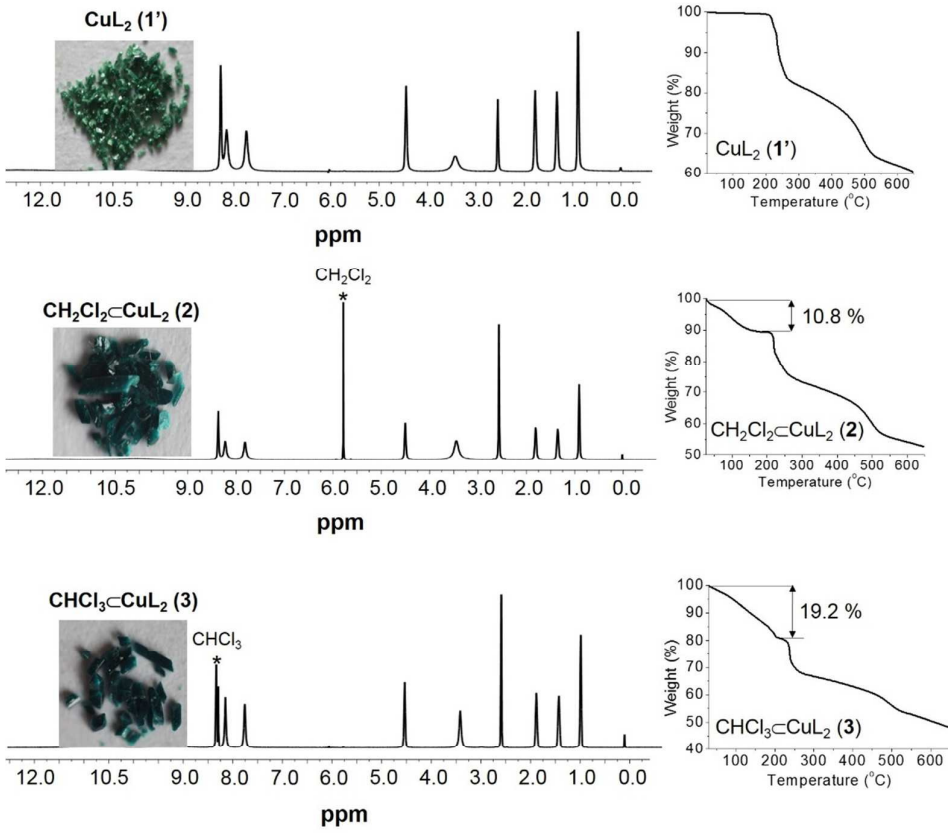

Figure 2. From top to bottom: ^{1}H NMR spectra and corresponding TGA traces of **1'**, **2** and **3**. The encapsulated CH_2Cl_2 (δ = 5.76 ppm) and $CHCl_3$ (δ = 8.32 ppm) signals are marked for clarity. As shown in the Figure, the colors of **2-3** are different from that of **1'**, which could be a color-responsive guest-uptake.

In addition, when the desolvated sample of **1'** was respectively immersed in CH_2Cl_2 and $CHCl_3$ for 2 days (no difference in adsorption amount was observed at the longer time) at ambient temperature, the chlorocarbons were taken inside to generate $1.32(CH_2Cl_2)\subset Cu\mathbf{L}_2$ (**2**) and $1.84(CHCl_3)\subset Cu\mathbf{L}_2$ (**3**). Unfortunately, compounds **2** and **3** cannot keep their single-crystal nature during the chlorocarbons adsorption process although the crystal shape was maintained (Figure 2). The guest uptake, however, can be clearly determined by the ^{1}H NMR and TGA analysis. As shown in Figure 2, the ^{1}H NMR spectra of **2-3** indicated the chlorocarbons are present in the

channels, and the adsorption amounts of CH_2Cl_2 and $CHCl_3$ are up to 10.8 and 19.2 % respectively based on TGA measurements (Figure 2). The PXRD patterns of **2-3** indicated that the framework of **1** was retained in the processes of the chlorocarbons adsorption (Supporting Information). The chlorocarbon-free framework of **1'** can be further regenerated by solid-liquid extraction with acetonitrile (Supporting Information). So the chlorocarbons adsorption based on Cu**L**$_2$ framework is reversible. In addition, the Cu**L**$_2$ framework cannot upload CCl_4 under the same conditions which was demonstrated by the ^{13}C NMR and TGA measurement (Supporting Information). At this stage, we have to say forthright that we cannot explain this adsorption behavior for CCl_4, but the Cu**L**$_2$ framework can be a useful separator to naturally isolate CCl_4 from CH_2Cl_2 and $CHCl_3$.

As shown above, the -ABAB- stacking of the layers in **1** generates reduced, yet still large infinite channels of dimensions ca. 12 × 12 Å. Such void space should be suitable for accommodation of BTEX according to our previous study.[6m-n] It is noteworthy that the adsorption capacity for BTEX based on the evacuated framework of Cu**L**$_2$ (**1'**) is lower in comparison with the guest-loaded compound of CH_2Cl_2⊂Cu**L**$_2$ (**2**). For example, when the crystals of **1'** were soaked in benzene for 2 days to generate 0.29(benzene)⊂Cu**L**$_2$ (based on ^1H NMR measurement), meanwhile the benzene uptake increased and 0.67(benzene)⊂Cu**L**$_2$ was obtained when **2** was used for benzene sorption via guest-exchange approach. Although we say forthright that we currently cannot well demonstrate such phenomenon in detail, we believe that

the different orientations of the n-butyl groups of **1'** and **2** might play an important role in the benzene adsorption. So the BTEX uptake was carried out based on **2**. When the crystalline solids of **2** were respectively immersed in benzene, toluene, ethylbenzene, *o*-, *m*-, and *p*-xylene for 2 days, the corresponding ^{1}H NMR spectra indicated that all the compounds can be uploaded (Figure 3). TGA analysis indicated that the uploaded amounts of benzene, toluene, ethylbenzene, *o*-, *m*-, and *p*-xylene are up to 6.2, 8.8, 12.5, 15.3, 9.6 and 13.2 %, respectively, which is well consistent with the ^{1}H NMR measurement (Figure 3). So the formula of new host-guest complexes can be shown as 0.67(benzene)⊂Cu**L**$_2$ (**4**), toluene⊂Cu**L**$_2$ (**5**), 1.1(ethylbenzene)⊂Cu**L**$_2$ (**6**), 1.6(*o*-xylene)⊂Cu**L**$_2$ (**7**), *m*-xylene⊂CuL$_2$ (**8**), 1.3(*p*-xylene)⊂Cu**L**$_2$ (**9**), respectively. On the other hand, the uploaded guest molecules can be further removed by solid-liquid extracting (by CD_3CN) to regenerate the guest-free framework, which is confirmed by the ^{1}H NMR spectra (Supporting Information). So the porous Cu**L**$_2$ is a recyclable absorbent for BTEX at this point. Unfortunately, the framework can hardly trap C_9-aromatics such as mesitylene clearly due to the pore size limitation (Supporting Information).

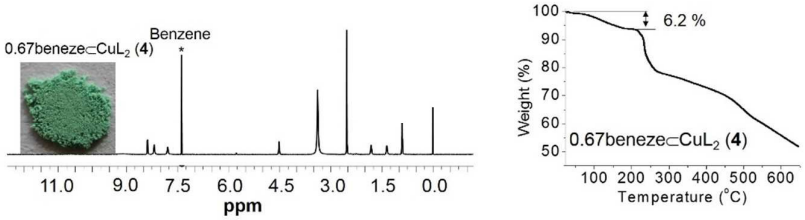

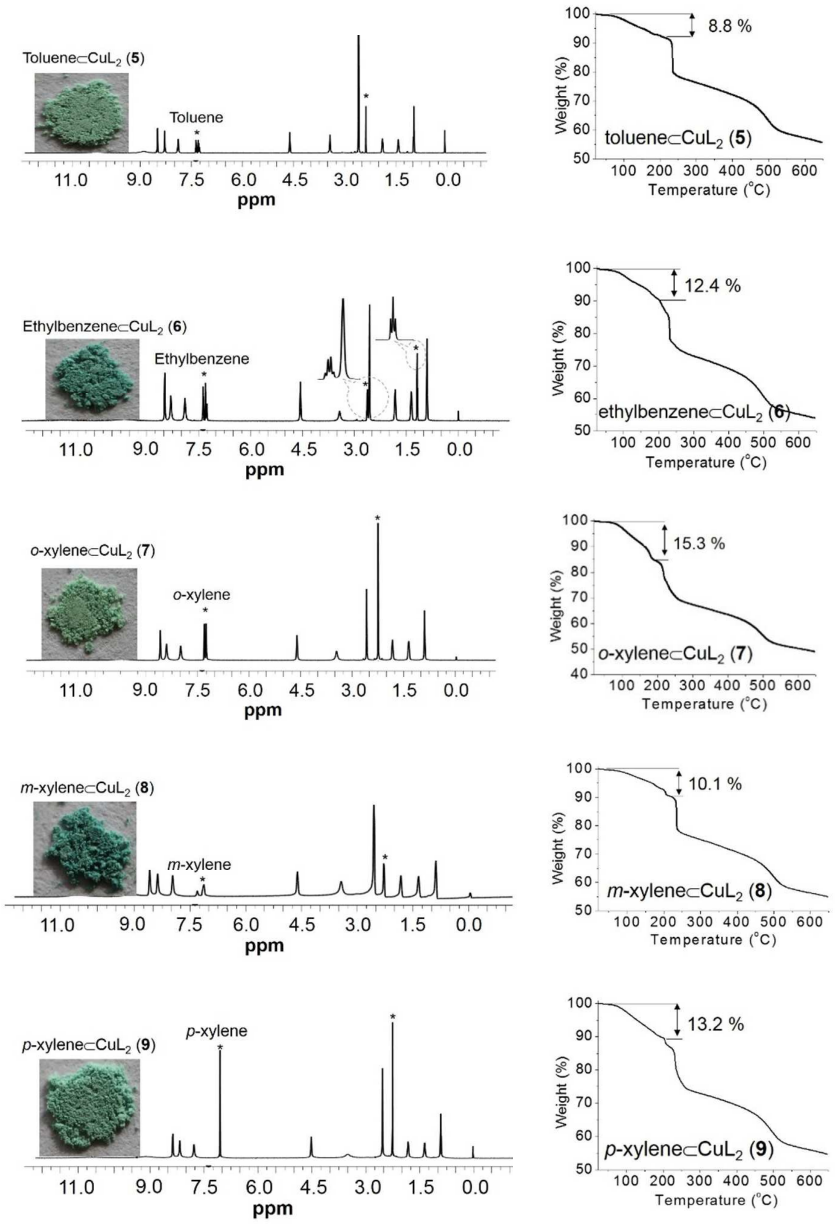

Figure 3. From top to bottom: ^{1}H NMR (DMSO-d^{6}) spectra and corresponding TGA traces of **4-9**. The corresponding signals of the uploaded BTEX guest are marked for clarity. The photographs of sample of **4-9** are inserted. As shown in the Figure, the colors of **4-9** are slightly different, which could be a color-responsive guest-uptake.

Chlorocarbons separation

As we known, the major hurdle in molecular separation is guest selectivity for capturing a specific substrate in the presence of one or several different potential

competitors. In principle, suitable MOFs constructed by the rational combination of subtly designed organic ligands and metal ions are able to selectively absorb one type of chlorocarbons in the presence of other kinds of homologues. Because CCl_4 molecule is not able to enter the pores of **1'**, so the affinity for chlorocarbons was examined in a competitive batch experiment using a bicomponent sample of CH_2Cl_2 and $CHCl_3$. When the crystalline solids of **1'** were immersed in a mixed solvent of CH_2Cl_2 and $CHCl_3$ (molar ratio 1:1) at ambient temperature for 2 days (no difference in binding was observed at the longer time), ^{1}H NMR spectrum performed on the CD_3CN extract clearly evidenced that only the $CHCl_3$ (single peak at 7.58 ppm) was taken up by the Cu**L**$_2$ framework, and no CH_2Cl_2 species was simultaneously uploaded (Figure 4). Compared to ^{1}H NMR characterization, the corresponding CH_2Cl_2 impurity was detected by the GC analysis due to its lower detection limit. As shown in Figure 4, the GC peak area ratio between $CHCl_3$ and CH_2Cl_2 is 27.8 : 1. So the larger-sized $CHCl_3$ is the preferred guest for the Cu**L**$_2$ framework instead of the smaller-sized CH_2Cl_2. On the other hand, the polarity of these two chlorocarbons increases following a sequence of $CHCl_3$ (ε = 4.86, μ = 1.04 D) < CH_2Cl_2 (ε = 8.65, μ = 1.60 D),[9] which is opposite to that of affinity. Thus, the affinity and strict selectivity of these chlorocarbons binding in **1'** might mainly result from the polarity of the substrates instead of size and shape, which is different from our previous observation.[6l]

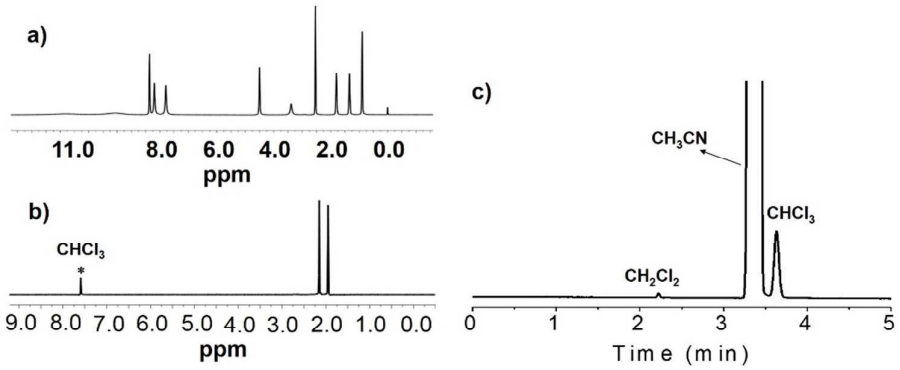

Figure 4. a) ^{1}H NMR (DMSO-d^6) spectrum of the desolvated sample after CD_3CN extraction. No chloroform signal (δ = 8.32 ppm) is found in the spectrum. b) ^{1}H NMR (CD_3CN) spectrum performed on the CD_3CN extract. The corresponding chloroform signal (δ = 7.58 ppm) is marked, and no peak related to CH_2Cl_2 was found in the spectrum. c) GC analysis result performed on the CD_3CN extract.

BETX separation

As shown above, compound **2** is able to upload BTEX via guest-exchange along with the different sorption amounts, so we wonder if it can used to separate BTEX in liquid phase under ambient conditions. Combined with the fact that the adsorption amounts of benzene and toluene are smaller than those of ethylbenzene and xylene, the focus will be on the separation of benzene from toluene/ethylbenzene/xylene and toluene from ethylbenzene/xylene. The separation ability of **2** was examined by soaking of crystalline solids of **2** in the corresponding mixed systems consisting of equimolar amounts of BTEX species. After 2 days (no difference was detected at longer time), the resulted guest loading samples were extracted by CD_3CN and the acetonitrile extracts were analyzed by GC (Table 3).

Table 3. BTEX separation based on **2**.

BTEX systems	GC peak area ratios	BTEX systems	GC peak area ratios
benzene/toluene 1 : 1	benzene : toluene 1 : 19.35	toluene/*m*-xylene 1 : 1	toluene : *m*-xylene 1 : 3.02
benzene/ethylbenzene 1 : 1	benzene : ethylbenzene 1 : 72.34	toluene/*p*-xylene 1 : 1	toluene : *p*-xylene 1 : 26.64
benzene/*o*-xylene 1 : 1	benzene : *o*-xylene 1 : 24.60	benzene/toluene/*o*-xylene 1 : 1 : 1	benzene : toluene: *o*-xylene 1 : 3.47 : 21.72
benzene/*m*-xylene 1 : 1	benzene : *m*-xylene 1 : 45.29	benzene/toluene/*m*-xylene 1 : 1 : 1	benzene : toluene : *m*-xylene 0 : 1: 12.90
benzene/*p*-xylene 1 : 1	benzene : *p*-xylene 1 : 161.90	benzene/toluene/*p*-xylene 1 : 1 : 1	benzene : toluene : *p*-xylene 1 : 10.03 : 82.59
toluene/ethylbenzene 1 : 1	toluene : ethylbenzene 1 : 8.66	benzene/toluene/ethylbenzene 1 : 1 : 1	benzene : toluene : ethylbenzene 0 : 0 : 1
toluene/*o*-xylene 1 : 1	toluene : *o*-xylene 1 : 6.95		

As indicated in Table 3, compound **2** is able to effectively separate benzene or toluene from its larger-sized aromatic analogues. For instance, the bicomponent competitive experiments indicated that the sorption amounts of C_7-C_8 aromatics are 19.35-161.90 times than that of benzene, while the sorption amounts of C_8-aromatics are 3.02-26.64 times than that of toluene. In the case of tricompontent competitive experiments, the observation is quite similar to those of bicomponent ones. For benzene/toluene/xylene (1 : 1 : 1), the affinity for these competitors follows a sequence of xylene > toluene > benzene. For benzene/toluene/ethylbenzene (1 : 1 : 1), it seems surprising that the much smaller-sized benzene and toluene even cannot get into pores based on the GC analysis and ^{1}H NMR characterization (Figure 5).

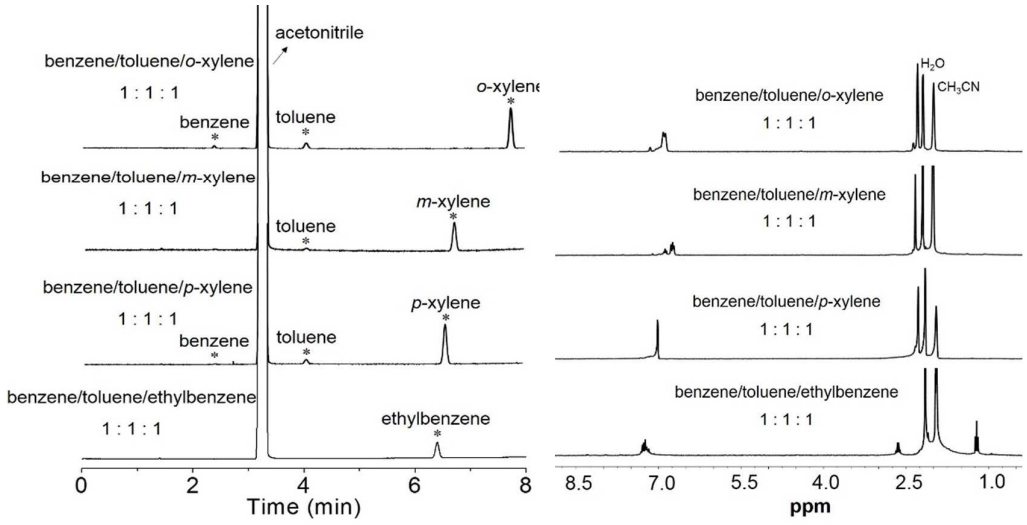

Figure 5. Left: GC analysis performed on the CD_3CN extracts for tricomponent samples based on **2**. Right: the corresponding ^1H NMR spectra performed on the CD_3CN extract for tricomponent samples based on **2**.

Based on above discussion, the most notable observation is that the larger-sized xylene or ethylbenzene species is preferred much more than the co-existed smaller-sized benzene and toluene, which is remarkably different from those guest-dimension controlled selectivity.[6] On the other hand, it does not seem possible at present to explain the affinity preference for BTEX based on the molecular polarity (benzene $\varepsilon = 2.3$, $\mu = 0$ D; toluene $\varepsilon = 2.4$, $\mu = 0.43$ D; ethylbenzene $\varepsilon = 2.4$, $\mu = 0.36$ D; *o*-xylene $\varepsilon = 2.6$, $\mu = 0.51$ D; *m*-xylene $\varepsilon = 2.4$, $\mu = 0.30$ D; *p*-xylene $\varepsilon = 2.3$, $\mu = 0$ D).[10] In light of the Cu**L**$_2$ structural feature and the above GC analysis data, we postulated that this rigorous selectivity for BTEX is primarily governed by lipophilic effect. Obviously, the above results show that the amount of BTEX bound to the framework increases in the order alkylaromatics > benzene and more alkyl-branched aromatics > toluene. As we know, the strength of hydrophobic interaction per alkyl

side group follows the order -C_2H_5 > -CH_3.[11] Accordingly, it could be concluded that BTEX might be encapsulated in the n-C_4H_9-filled pores due to hydrophobic interactions.

Conclusions

In summary, through this work, the synthesis of a new carbazole-bridged ligand **L** with n-butyl group, and a new copper(II) porous metal-organic framework Cu**L**$_2$(NO_3)$_2$ (**1**), derived from it have been described. The ligand **L** together with Cu(II) nodes produce the 2D nets which further stack together to generate square-like channels. Notably, all the n-butyl groups on the ligands face toward channel center to form typical hydrophobic pores. It can reversibly adsorb some VOCs such as CH_2Cl_2/$CHCl_3$ and BTEX, furthermore effectively separate them in the presence of other competitors in liquid phase. For chlorocarbons, the rigorous selectivity shown by the Cu(II)-MOF is mainly derived from the molecular polarity. For BTEX, the dominating factor for selectivity might be the host-guest hydrophobic interactions instead of size, shape and even polarity.

Acknowledgement

We are grateful for financial support from NSFC (Grant Nos. 21271120, 21475078 and 21101100), 973 Program (Grant Nos. 2012CB821705 and 2013CB933800) and the Taishan scholar's construction project.

†**Electronic supporting information.** The ORTEP figure of **1**, X-ray crystallographic details in CIF format, corresponding TGA traces, XRPD patterns, NMR spectra.

CCDC 1054563. For ESI and crystallographic data in CIF or other electronic format see DOI:

‡ These authors contributed equally.

Notes and references

1 R. G. Prinn, R. F. Weiss, P. J. Fraser, P. G. Simmonds, D. M. Cunnold, F. N. Alyea, S. O'Doherty, P. Salameh, B. R. Miller, J. Huang, R. H. J. Wang, D. E. Hartley, C. Harth, L. P. Steele, G. Sturrock, P. M. Midgley, McCulloch, A. *Journal of Geophysical Research*, 2000, **105**, 17751.

2 (a) D. E. Reusser, J. D. Istok, H. R. Beller, J. A. Field, *Environ. Sci. Technol.* 2002, **36,** 4127. (b) S. B. Hawthorne, D. J. Miller, *Environ. Sci. Technol.* 2003, **37**, 3587. (c) Y. Ueno, T. Horiuchi, T. Morimoto, O. Niwa, *Anal. Chem*. 2001, **73**, 4688.

3 J. Wu, H. Zhao, Z. Wang, *Adsorption Science & Technology*, 2002, **20**, 169.

4 (a) J.-R. Li, J. Sculley, H.-C. Zhou, *Chem. Rev.* 2012, **112**, 869. (b) H. Wu, Q. Gong, D. H. Olson, J. Li, *Chem. Rev.* 2012, **112**, 836. (c) K. Sumida, D. L. Rogow, J. A. Mason, T. M. McDonald, E. D. Bloch, Z. R. Herm, T.-H. Bae, J. R. Long, *Chem. Rev*. 2012, **112**, 724.

5 (a) N. Nijem, H. Wu, P. Canepa, A. Marti, K. J. Balkus, Jr, T. Thonhauser, J. Li, Y. J. Chabal, *J. Am. Chem. Soc.* 2012, **134**, 15201. (b) A. Shigematsu, T. Yamada, H. Kitagawa, *J. Am. Chem. Soc.* 2012, **134**, 13145. (c) M. C. Das,

Q. Guo, Y. He, J. Kim, C.-H. Zhou, K. Hong, S. Xiang, Z. Zhang, K. M. Thomas, R. Krishna, B. Chen, *J. Am. Chem. Soc.* 2012, **134**, 8703. (d) C.-T. He, J.-Y. Tian, S.-Y. Liu, G. Ouyang, J.-P. Zhang, X.-M. Chen, *Chem. Sci.* 2013, **4**, 351. (e) Y.-S. Bae, C. Y. Lee, K. C. Kim, O. K. Farha, P. Nickias, J. T. Hupp, S. T. Nguyen, R. Q. Snurr, *Angew. Chem. Int. Ed.* 2012, **51**, 1857.

6 (a) M. Maes, L. Alaerts, F. Vermoortele, R. Ameloot, S. Couck, V. Finsy, J. F. M. Denayer, D. E. De Vos, *J. Am. Chem. Soc.* 2010, **132**, 2284–2292. (b) R. E. Osta, A. Carlin-Sinclair, N. Guillou, R. I. Walton, F. Vermoortele, M. Maes, D. de Vos, F. Millange, *Chem. Mater.* 2012, **24**, 2781–2791. (c) G. Xu, X. Zhang, P. Guo, C. Pan, H. Zhang, C. Wang, *J. Am. Chem. Soc.* 2010, **132**, 3656–3657. (d) V. Finsy, H. Verelst, L. Alaerts, D. De Vos, P. A. Jacobs, G. V. Baron, J. F. M. Denayer, *J. Am. Chem. Soc*. 2008, **130**, 7110–7118. (e) M. Maes, F. Vermoortele, L. Alaerts, S. Couck, C. E. A. Kirschhock, J. F. M. Denayer, D. E. De Vos, *J. Am. Chem. Soc.* 2010, **132**, 15277–15285. (f) L. Alaerts, M. Maes, L. Giebeler, P. A. Jacobs, J. A. Martens, J. F. M. Denayer, C. E. A. Kirschhock, D. E. De Vos, *J. Am. Chem. Soc.* 2008, **130**, 14170–14178 (g) Q.-K. Liu, J.-P. Ma, Y.-B. Dong, *J. Am. Chem. Soc.* 2010, **132**, 7005–7017. (h) D. Liu, J.-P. Lang, B. F. *J. Am. Chem. Soc.* 2011, **133**, 11042–11045 (i) F. Vermoortele, M. Maes, P. Z. Moghadam, M. J. Lennox, F. Ragon, M. Boulhout, S. Biswas, K. G. M. Laurier, I. Beurroies, R. Denoyel, M. Roeffaers, N. Stock, T. Düren, C. Serre, D. E. De Vos, *J. Am. Chem. Soc*. 2011, **133**, 18526–18529 (j) L. Wang, Y.-A. Li, F. Yang, Q.-K. Liu,

J.-P. Ma, Y.-B. Dong, *Inorg. Chem*. 2014, **53**, 9087–9094 (k) L. Duan, Z.-H. Wu, J.-P. Ma, X.-W. Wu, Y.-B. Dong, *Inorg. Chem.* 2010, **49**, 11164–11173 (l) Q.-K. Liu, J.-P. Ma, Y.-B. Dong, *Chem. Commun.* 2011, **47**, 12343-12345 (m) Q.-K. Liu, J.-P. Ma, Y.-B. Dong, *Chem. Eur. J.* 2009, **15**, 10364-10368. (n) J.-Y. Cheng, P. Wang, J.-P. Ma, Q.-K. Liu, Y.-B. Dong, *Chem. Commun.* 2014, **50**, 13672-13675.

7 CrysAlisPro, Agilent Technologies,Version 1.171.36.32 (release 02-08-2013 CrysAlis171. NET). Empiricalabsorption correction using spherical harmonics, implemented in SCALE3 ABSPACK scaling algorithm.

8 G. M. Sheldrick, *Acta Crystallogr*. 2008, **A64**, 112-122.

9 J. Joo, J. K. Lee, J. K. Hong, J. S. Baeck, W. P. Lee, A. J. Epstein, K. S. Jang, J. S. Suh, E. J. Oh, *Macromolecules*, 1998, **31**, 479.

10 (a) C. L. Yaws, *Chem. Eng*. 1975, **21**, 113. (b) C. L. Yaws, *Chem. Eng*. **1975**, **29**, 73. (c) Kirk-Othmer Encyclopedia of Chemical Technology, Copyright © 1999-2014 by John Wiley and Sons, Inc.

11 S. Miyamoto, *Macromolecules* 1981, **14**, 1054.

For table content

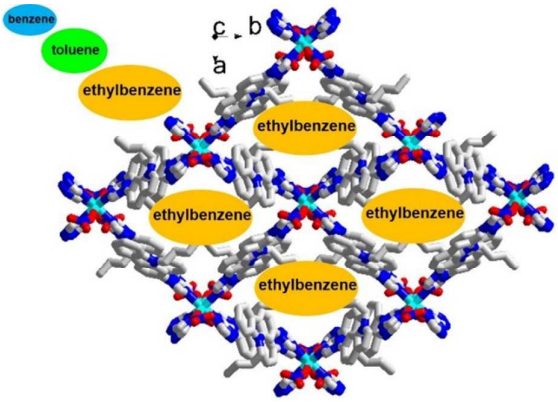

A new porous Cu(II)-MOF which is able to effectively separate VOCs such as chlorocarbons or BTEX is reported.